PARRACHA J.L., BORSOI G., FLORES-COLEN I., VEIGA R., NUNES N., DIONÍSIO A., GLÓRIA GOMES M., FARIA P. (2021), Performance parameters of ETICS: Correlating water resistance, bio-susceptibility and surface properties. Construction and Building Materials 272 (February 2021), 121956. https://doi.org/10.1016/j.conbuildmat.2020.121956

Performance parameters of ETICS: Correlating water resistance, bio-susceptibility and surface properties

J. L. Parracha[1,2*], G. Borsoi[2], I. Flores-Colen[2], R. Veiga[1], L. Nunes[1,3], A. Dionísio[4], M. Glória Gomes[2], P. Faria[5]

[1]National Laboratory for Civil Engineering, Av. do Brasil, 101, 1700-066, Lisbon, Portugal

[2]CERIS, DECivil, Instituto Superior Técnico, University of Lisbon, Av. Rovisco Pais, 1049-001, Lisbon, Portugal

[3]cE3c, Centre for Ecology, Evolution and Environmental Changes, Azorean Biodiversity Group, University of Azores, 9700-042, Angra do Heroísmo, Azores, Portugal

[4]CERENA, DECivil, Instituto Superior Técnico, University of Lisbon, Av. Rovisco Pais, 1049-001, Lisbon, Portugal

[5]CERIS and DEC, School of Science and Technology, NOVA University of Lisbon, 2829-516, Caparica, Portugal

*Corresponding author

E-mail address: jparracha@lnec.pt (J.L. Parracha); Phone: +351 218443298

ABSTRACT

The use of External Thermal Insulation Composite Systems (ETICS) significantly increased in the last decades due to their enhanced thermal properties, low installation cost and ease of application, not only in new constructions but also for thermal retrofitting of building facades. These multilayer rendering systems are constantly exposed to weathering agents and anthropic factors which can lead to physical-mechanical and aesthetical anomalies and thus affect their durability. However, possible synergetic effects among these agents are often neglected by international technical documents on the evaluation of the effectiveness and durability of ETICS. With the aim of filling this gap, moisture transport properties (capillary water absorption, water vapor permeability, water absorption under low pressure, and drying kinetics), thermal conductivity, mould susceptibility and surface properties (color, gloss, and roughness) of twelve commercially available ETICS were assessed and discussed. Possible links between these factors were analyzed and ETICS performance parameters were defined. Results demonstrate that a deeper knowledge of the correlation among ETICS properties can effectively contribute to the evaluation of the efficiency and long-term durability of these systems.

Keywords: ETICS; Moisture transport; Surface properties; Thermal conductivity; Mould susceptibility; Performance parameters

Nomenclature

A – Specimen's area [m^2]

a^* - Red/green coordinate, according to CIELAB color space

A_{bp} – Mass of water absorbed at 60 min [kg]

$A_{contact}$ – Contact area of the tube with the surface [m^2]

b^* - Yellow/blue coordinate, according to CIELAB color space

BC – Base coat

C^*_{ab} – Chroma or color saturation

C_{abs} – Water absorption coefficient (Karsten tubes) [$kg/(m^2.min^{0.5})$]

C – Capillary water absorption coefficient [$kg/(m^2.min^{0.5})$]

$DR1$ – First drying rate [$kg/(m^2.h)$]

$DR2$ – Second drying rate [$kg/(m^2.h^{0.5})$]

e – Specimen's thickness [m]

EPS – Expanded polystyrene

ETICS – External Thermal Insulation Composite System

FC – Finishing coat

ICB – Expanded cork agglomerate

L^* - Luminosity coordinate, according to CIELAB color space

m – Slope of the linear correlation between mass variation and time [kg/s]

MS1 – Moisture state 1 [%]

MS2 – Moisture state 2 [%]

MW – Mineral wool

RS – Rendering system

S_d – Equivalent air thickness [m]

TI – Thermal insulation

Greek letters

Δ_p – Difference between the exterior and interior vapor pressure [Pa]

λ_{DS} – Thermal conductivity for dry state [W/(m.K)]

λ_{MS1} – Thermal conductivity for moisture state 1 [W/(m.K)]

λ_{MS2} – Thermal conductivity for moisture state 2 [W/(m.K)]

Λ - Water vapor permeance [$kg/(m^2.s.Pa)$]

μ - Water vapor diffusion resistance coefficient

Ψ – Moisture content [%]

1. Introduction

External Thermal Insulation Composite Systems (ETICS) are multilayer solutions with enhanced thermal properties which are applied to building facades. These systems are generally composed of three layers: the thermal insulation (TI), fixed to the building external wall; the base coat, which incorporates at least one glass fiber mesh as reinforcement; and the finishing coat. Expanded polystyrene (EPS), extruded polystyrene (XPS), mineral wool (MW) and expanded cork (ICB) are among the most widely used thermal insulation board materials for these solutions [1,2], being EPS and MW the most common TI adopted for ETICS in Europe [3]. The base coat is formed by a mortar with several possible formulations, with a hydraulic binder, fillers, and mineral or organic additives (resins, fibres, among others). The finishing coat generally consists of a key-coat and a thick plastic coating or a paint (e.g. acrylic or silicate-based). These solutions usually provide enhanced water repellant properties, decreasing the liquid water permeability of the base coat [4], thus preventing water to achieve the thermal insulation layer. In fact, several studies [5-8,58] reported that the thermal conductivity of different construction materials increases with their moisture content. Hence, a suitable protection to the rendering system (RS), i.e. the combination of the base coat (BC) and the finishing coat (FC), against water penetration and the main degradation agents (wind-driven rain, solar radiation, biocolonization, among others) can increase ETICS performance and their service life, beyond the 25 years required by the Guideline for European Technical Approval of External Thermal Insulation Composite Systems with Rendering – ETAG 004 [9].

The use of ETICS in new constructions and building facades' thermal retrofitting significantly increased over the last decades due to their performance characteristics, as well as to the introduction of new international and national regulations on building energy efficiency [2,3,10,11]. ETICS have several advantages when compared with other thermal insulation solutions. Besides contributing to increase the level of insulation of the building thermal envelope, thus reducing building environmental impact throughout its service life, ETICS also mitigate thermal bridges, protect the masonry and structural elements from thermal stress and moisture and reduce interior water condensation within masonry. Additionally, these systems present relatively low installation cost and ease of application [12-15]. Nevertheless, ETICS' still have several disadvantages, such as the occurrence of biological growth [12,16,17], loss of adherence between the different components of the system [1,18], low impact resistance [19] and color change [20], which can limit their performance and, therefore, a wider diffusion of this technology.

Biological growth has been identified in several ETICS facades only few years after the building construction or retrofitting [12,16]. Even though it might not have major influence on the ETICS thermal performance, it causes cladding defacement, by altering the aesthetic appearance of the building, and thus leading to the disapproval of building owners with regards to the use of ETICS. Previous studies [17,21,22] showed that biological growth is strongly influenced by the surface properties (e.g. temperature, relative humidity, pH, roughness) of the finishing coat, being hygroscopicity a key factor. In fact, extensive mould development is linked to high levels of surface moisture content, resulting from the combined effect of surface condensation, wind-driven rain, drying process and rendering properties [12,17], in turn depending on mortar composition. Surface condensation occurs whenever the external surface temperature is lower than the dew point temperature of the air [12]. Additionally, when the drying process is slow, the surface moisture content remains high for long periods, increasing the risk of biocolonization. Previous studies also address the importance of rendering properties in the biological development [12,17,74]. As an example, lower values of emissivity lead to an increased surface temperature, caused by a reduction of the heat loss during the night, and therefore lower risk of surface condensation [12,74]. Barberousse et al. [21] also concluded that high surface roughness promotes high liquid water retention and facilitates the spores adhesion to the surface, leading to a higher risk of biological growth. Other complex and synergetic factors influencing mould growth on ETICS include nutrient availability, environmental conditions and exposure time.

The European guideline ETAG 004 [9] provides requirements and test methods for the evaluation of ETICS performance. ETAG 004 considers ETICS' systems as a whole in terms of the definition of performance requirements and testing; however, it provides no correlation among the established requirements and components characteristics. This implies that, when a component is changed, all the system needs to be evaluated again as a whole [1]. Furthermore, according to ETAG 004 all system components should maintain their properties during the overall service life of ETICS under normal maintenance conditions. Nevertheless, no requirements and test methods are considered to evaluate and monitor ETICS resistance to biocolonization. In summary, ETICS are constantly exposed to weathering agents and anthropic factors which can lead to physical-mechanical and aesthetical anomalies and thus affect their durability. However, possible synergetic effects among these agents are often neglected by international technical documents on the evaluation of the effectiveness and durability of ETICS. Hence, further knowledge of the moisture transport properties, the moisture dependence of the thermal conductivity, the bio-susceptibility, and the surface properties can

effectively contribute to the evaluation of the efficiency and long-term durability of ETICS, addressing the importance of a holistic view for the correct evaluation of these systems. Moreover, the effective contribution of the characteristics of each component on the overall performance of the system is another gap in the present knowledge.

This paper aims at evaluating the water resistance, bio-susceptibility and surface properties of different commercially available ETICS, focusing on the role of each type of component. The influence of the moisture content variation on the thermal conductivity of the insulation layer of ETICS was also investigated. Correlations among these properties were described, defining ETICS performance parameters that can be used in combination with the requirements provided in ETAG 004 [9]. Ultimately, this work contributes towards the development and implementation of ETICS with improved effectiveness and durability in the urban environment.

2. Materials and methods

2.1. Materials

Twelve different commercially available ETICS' systems (S), supplied by three different manufacturers, were tested. The identification, composition and thickness of each system is presented in Table 1 and Figure 1. The selected systems are certified and have European Technical Assessment (ETA), thus they can be considered as systems of suitable quality and adequate performance.

Table 1. Identification, composition and thickness of ETICS and their components

<table>
<tr><th rowspan="2">System (S)</th><th rowspan="2">Thermal insulation (TI)</th><th colspan="2">Rendering system (RS)</th><th colspan="3">Thickness [mm]</th></tr>
<tr><th>Base coat (BC)*</th><th>Finishing coat (FC)</th><th>S (total)</th><th>TI</th><th>RS</th></tr>
<tr><td>S1</td><td rowspan="3">EPS</td><td rowspan="3">Cement, synthetic resins, mineral additives</td><td>Key-coat: water-based dispersion of acrylic co-polymer
Finishing: acrylic paint, quartz aggregates and additives</td><td>39.87</td><td>36.66</td><td>3.21</td></tr>
<tr><td>S2</td><td>Key-coat: water-based acrylic dispersion
Finishing: a) water-based acrylic co-polymer, pigments and marble powder; b) water-based acrylic paint and additives</td><td>40.57</td><td>37.70</td><td>2.87</td></tr>
<tr><td>S3</td><td>Key-coat: water-based acrylic dispersion
Finishing: water-based acrylic co-polymer, pigments, marble powder and additives</td><td>40.27</td><td>37.55</td><td>2.72</td></tr>
<tr><td>S4</td><td rowspan="2">ICB</td><td rowspan="3">Natural hydraulic lime, cement, mineral fillers, resins and synthetic fibres</td><td>Air lime, hydraulic binder and organic additives</td><td>65.85</td><td>58.83</td><td>7.02</td></tr>
<tr><td>S5</td><td rowspan="2">Key-coat: acrylic co-polymer and mineral additives
Finishing: acrylic paint, mineral aggregates, pigments and additives</td><td>64.15</td><td>60.50</td><td>3.65</td></tr>
<tr><td>S6</td><td>EPS</td><td></td><td>65.45</td><td>59.77</td><td>5.68</td></tr>
</table>

S7		Cement, mineral fillers, resins and synthetic fibres	Key-coat: acrylic co-polymer and mineral aggregate Finishing: acrylic paint, organic additives and pigments	64.53	59.99	4.54
S8	MW		Key-coat: acrylic co-polymer and mineral additives Finishing: acrylic paint, mineral aggregates, pigments and additives	61.34	56.83	4.51
S9	ICB	Natural hydraulic lime, mixed binders and cork aggregates	Key-coat: water-based dispersion of silicate Finishing: water-based silicate paint, organic additives and pigments	43.91	38.57	5.34
S10			Key-coat: acrylic dispersion and mineral aggregate Finishing: acrylic paint, siloxane resin and marble powder	41.91	37.52	4.39
S11	EPS	Cement, natural hydraulic lime and aggregates		43.30	38.51	4.79
S12	MW			44.77	39.93	4.84
EPS – expanded polystyrene; ICB – expanded cork agglomerate; MW – mineral wool board; *Includes a standard or reinforced glass fiber mesh						

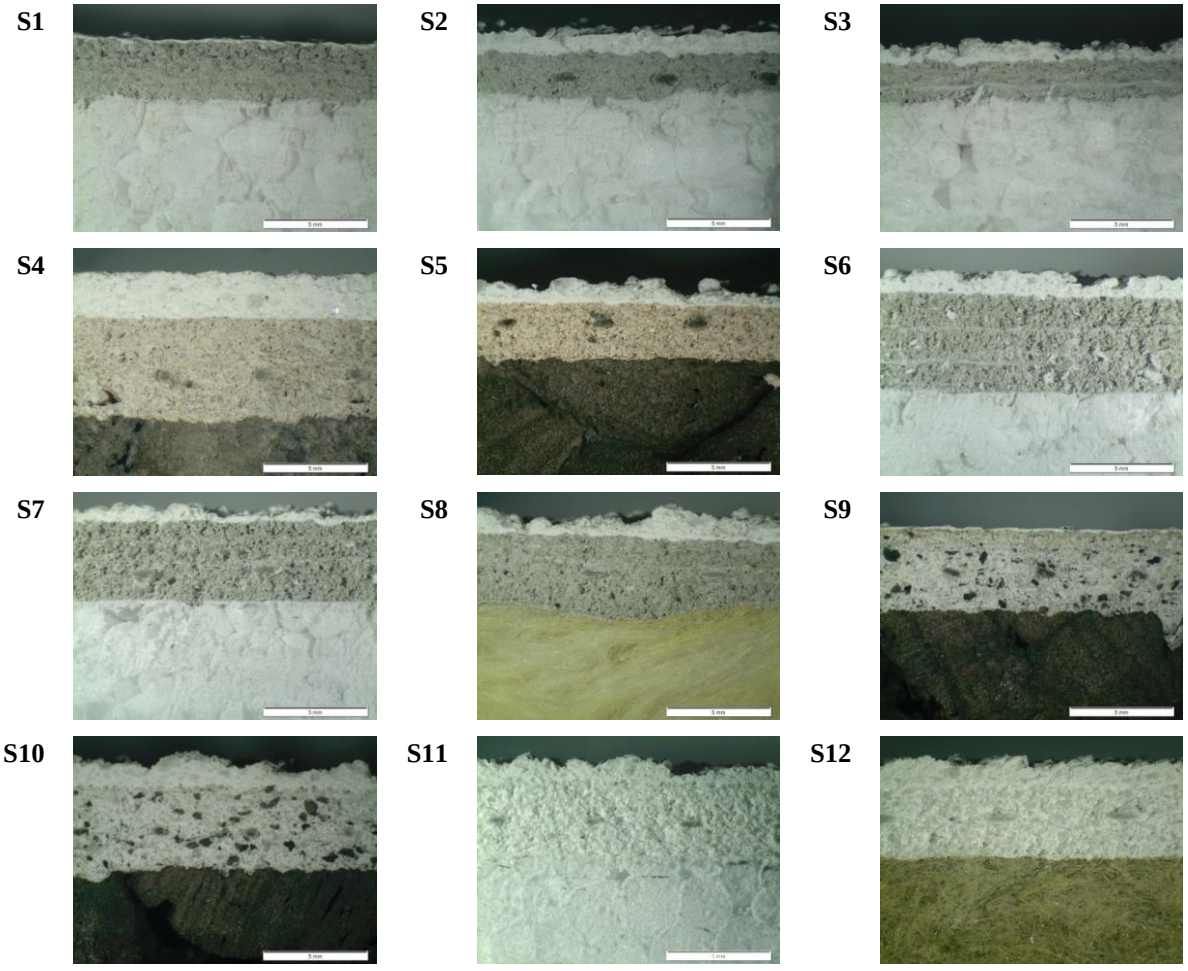

Figure 1. Microphotographs of the cross section of the different systems

Specimens with different dimensions and shapes were used, according to the tests performed, as resumed in Table 2. Additionally, the thermal insulation materials (TI) of the systems were also individually tested for mould growth, in order to assess the influence of the TI composition on the ETICS performance. The

dimensions of these specimens are 40 mm × 40 mm × TI thickness (Table 1) and three specimens of each system were tested.

Table 2. Characterization tests performed and sampling

Test		Reference	Sampling [Specimens × S]	Dimensions [mm]
Water performance	Capillary absorption and drying	ETAG 004 [9] and EN 16322 [23]	2 × 12	150 × 150 × S thickness
	Water vapor permeability	ETAG 004 [9] and EN 1015-19 [24]	3 × 12	Cylindrical with ø ~ 70
	Water absorption under low pressure	LNEC FE Pa 39 [25], RILEM [26] and EN 16302 [27]	2 × 12 (using 2 tubes per specimen)	150 × 150 × S thickness
Surface properties	Color and gloss	ASTM D2244 [28] and ASTM D6578 [29]	3 × 12 (4 and 9 values per specimen for color and gloss, respectively)	50 × 50 × S thickness
	Roughness	-	3 × 12 (9 values per specimen)	50 × 50 × S thickness
Thermal conductivity		ASTM D5930-09 [30] and equipment manual [31]	2 × 12 (the same used for capillary absorption and drying)	150 × 150 × S thickness
Biological susceptibility to moulds		ASTM D5590-17 [32] and ASTM C1338-19 [33]	3 × 12	40 × 40 × S thickness

All systems' surfaces were submitted to a preliminary visual and microscopic observation for anomalies detection. No cracking, loss of paint or surface irregularities were detected on the systems' surfaces.

2.2. Methods

2.2.1. Water performance

Water absorption by capillarity test was performed in a conditioned room with a temperature (T) of 23 ± 2 ºC and a relative humidity (RH) of 65 ± 5 %. Specimens were previously placed at these conditions for a period of 7 days for mass stabilization and laterally sealed using a metallic scotch tape, thus guaranteeing no direct contact between the water and the TI. The exterior surface of the specimens was then placed in direct contact with the water at a depth (approximately 3 mm) that ensures total submergence of the FC layer. In order to monitor mass variation due to water absorption, specimens were weighed at given time intervals (3 min, 1 h, 4 h, 8 h and 24 h).

The capillary water absorption coefficient (C in kg/(m^2.$min^{0.5}$)) characterizes the initial rate of liquid water absorption due to the capillary force of porous materials, and is obtained by the slope of the initial phase of the

capillary absorption curve, based on a linear regression, that expresses the mass of absorbed water (kg/m^2) as a function of the square root of time (min$^{0.5}$). The total amount of absorbed water at 1 h and 24 h was also assessed. According to ETAG 004 [9] the water absorption of the ETICS at 1 h should be lower than 1 kg/m^2. Furthermore, if this value is lower than 0.5 kg/m^2 at 24 h, no further assessment through freeze/thaw cycles is required to respect the guideline requirements.

Drying test started immediately after the end of the capillarity water absorption, evaluating the drying kinetics by measuring the weight loss at given time intervals till stabilization. The test was conducted in a conditioned room (T = 23 ± 2 ºC and 65 ± 5 % HR).

According to EN 16322 [23], two drying rates can be calculated: the first drying rate (DR1 in kg/(m^2.h)) and the second drying rate (DR2 in kg/(m^2.h$^{0.5}$)). DR1 corresponds to liquid transport and is obtained by the negative slope of the initial linear section of the drying curve plotted with time in abscissa. DR2 mainly corresponds to vapor transport and is determined by the negative slope of the linear section of the drying curve plotted against the square root of time in abscissa. Both DR's are obtained considering a linear regression.

Water vapor permeability (WVP) test was carried out adopting the dry cup method, which implies the use of a desiccant. Specimens were previously sealed within a recipient partially filled with a desiccant ($CaCl_2$), leaving a small gap of air space between the desiccant and the TI layer. The lateral sides of the specimens were sealed with scotch tape and waterproofed with paraffin wax, and the FC was exposed to the external environment. The use of a desiccant provides RH ~ 0 % inside the cup [72]. The specimens were then placed in a climatic chamber at T = 23 ± 2 ºC and 50 ± 5 % RH. Hence, water vapor was forced from the external environment (~ 50 % RH) to the interior of the cup (~ 0 % RH), fluxing through the layers of the ETICS. Mass variation of the specimens was daily monitored till stabilization.

The water vapor diffusion resistance coefficient (μ) can be obtained by using the following equations [24]:

$$\Lambda = \frac{m}{A \times \Delta_p} \tag{1}$$

$$\mu = \frac{1.94 \times 10^{-10}}{\Lambda \times e} \tag{2}$$

in which Λ is the water vapor permeance (kg/(m^2.s.Pa)), m is the slope of the linear correlation between mass variation and time (kg/s), A is the specimen area (m^2), Δ_p is the difference between the exterior and interior vapor pressure (Pa), and e is the specimen's thickness (m). Besides μ, it is also important to obtain the

equivalent air thickness (S_d in m) for the RS, as per ETAG 004 [9]. This value can be determined using Equation 3.

$$S_d = \mu \times e \tag{3}$$

According to ETAG 004 [9], the WVP of the whole system is analyzed by considering the S_d of the RS (BC plus FC). The value of S_d should not be higher than 2 m or 1 m, depending if the system has a cellular plastic insulation material (as is the case of EPS) or mineral wool insulation, respectively. Moreover, ETAG 004 [9] recommends that the value of μ for the insulation material shall be declared.

Water absorption under low pressure was carried out using Karsten tubes. This quick and non-destructive test consists of measuring the liquid water permeability under low pressure and can be used as a support for better understanding the influence of hydrophobic properties on the surface protection and additionally to detect the presence of micro-cracking (which may not influence the capillary absorption but be evidence in water under pressure) [34]. Two Karsten tubes for horizontal surfaces were applied on each specimen, using a sealing adhesive on the interface between the bottom end of the tube and the specimen surface. Each graduated tube was then water-filled till reaching 10 ml of water, monitoring water absorption at 5, 10, 15, 30 min and 1, 2, 4, 6 and 24 h.

In accordance with the recommendations of RILEM [26], the water absorption coefficient at 1 h (C_{abs} in kg/(m^2.min$^{0.5}$)) was obtained using Equation 4.

$$C_{abs} = \frac{A_{bp} \times 10^{-3}}{A_{contact} \times 10^{-4} \times \sqrt{60}} \tag{4}$$

in which A_{bp} indicates the absorbed water mass at 1 h (kg) and $A_{contact}$ represents the contact area of the tube with the surface (corresponding to the inner diameter of the Karsten tube – 5.7 cm^2).

2.2.2. Surface properties

Color characterization tests were performed using a portable Chroma Meter Minolta CR-410 measuring the CIELAB values (L^*, a^*, b^*). In CIELAB color space [73], L^* is the luminosity coordinate, varying from 0 (black) to 100 (white), a^* is the red/green coordinate (+a^* is red and -a^* is green), and b^* is the yellow/blue coordinate (+b^* is yellow and -b^* is blue). Specimens were analyzed in four different spots (each value is an average of three consecutive measurements). The measurements were performed in specular component

included mode (SCI), using the illuminant D_{65} (which corresponds to average daylight illuminant including ultraviolet radiation) at observer angle of 2º, featuring 50 mm diameter area of measurement.

The chroma or color saturation (C_{ab}) is obtained following Equation 5:

$$C_{ab} = (a^{*2} + b^{*2})^{0.5} \quad (5)$$

Surface gloss was determined using a specular gloss meter Rhopoint Novo-Gloss Lite and a measurement geometry of 60º was considered. Specimens were analyzed in nine different spots, considering the average values and relative standard deviation.

Surface roughness was evaluated using an Elcometer 223 surface profile gauge. This device can measure the peak-to-valley of a surface up to 2 mm, with a resolution of 0.001 mm. As for surface gloss, nine measurements were collected in different spots of each specimen, considering average values and relative standard deviation.

2.2.3. Thermal conductivity

With the aim of assessing the influence of the moisture content variation on the thermal conductivity of the ETICS, the thermal conductivity of the thermal insulation of each system (Figure 2) was determined, comparing three different experimental conditions: the dry state, obtained after mass stabilization in a climatic chamber at 23 ± 2 ºC and 50 ± 5% RH; moisture state 1 (MS1) – after 24 h of capillary water absorption at 23 ± 2 ºC and 65 ± 5%; and moisture state 2 (MS2) – after 2 months of natural exposure (with repeated wet-drying cycles).

Figure 2. Thermal conductivity measurements on the thermal insulation surface layer

The gravimetric moisture content (Ψ) was determined for each moisture state (MS1 and MS2) following Equation 6, in which m_i is the mass at each moisture state (g) and m_0 is the mass at dry state (g).

$$\Psi = \frac{(m_i - m_0)}{m_0} \times 100 \quad (6)$$

Thermal conductivity was determined by using an Isomet 2114 [31] equipment that uses a transient test method, according to ASTM D5930-09 [30]. For this test, a surface probe API 210412 with 60 mm diameter was used. This probe requires a minimum thickness of the evaluated material ranging between 20 and 40 mm. As presented in Table 1, both total thicknesses and those of the thermal insulation layers of all systems are close or higher than 40 mm, thus being within the required conditions. Further details on the functioning of this test can be found in previous studies [7,35].

2.2.4. Biological susceptibility to moulds

The biological susceptibility of ETICS and insulation materials to mould growth was assessed using a method adapted from ASTM D5590-17 [32] and ATMS C1338-19 [33] and previously described by Santos et al. [36]. *Aspergillus niger* and *Penicillium funiculosum* were selected as representative biodeterioration agents. These species were chosen due to their widespread presence in interior and outdoor environments and commonly referenced in the literature and standards [32,37,38]. *A. niger* and *P. funiculosum* strains from the fungal culture collection of the National Laboratory for Civil Engineering (LNEC) were used to obtain a mixed fungal suspension. A volume of 2 ml of spore suspension was then uniformly applied on the surface of the previously sterilized specimens and controls and the surrounding culture media (4 % malt, 2 % agar). After inoculation, the test flasks were incubated in a climatic chamber at T = 22 ± 1 ºC and 70 ± 5% RH for a period of four weeks.

The controls were three replicates of Whatman nº 1 filter paper (45 mm diameter) that allowed the validation of the test [33]. Each week, the specimens were visually rated for mould growth using the scale defined in Table 3. At the end of the exposure time, specimens were removed from the flasks and the final percentage of contaminated surface (Table 3) was evaluated by combining visual and stereozoom observations, the latter using a stereo microscope Olympus B061.

Table 3. Rate of mould development as defined in ASTM D5590-17 [32]

Rating	Description	Contaminated surface [%]
0	None	0%
1	Traces of growth	<10%
2	Light growth	10 to 30%
3	Moderate growth	30 to 60 %
4	Heavy growth	>60%

3. Results and discussion

3.1. Capillary absorption and drying

The results for capillary water absorption and drying are shown in Figures 3 and 4, and Table 4.

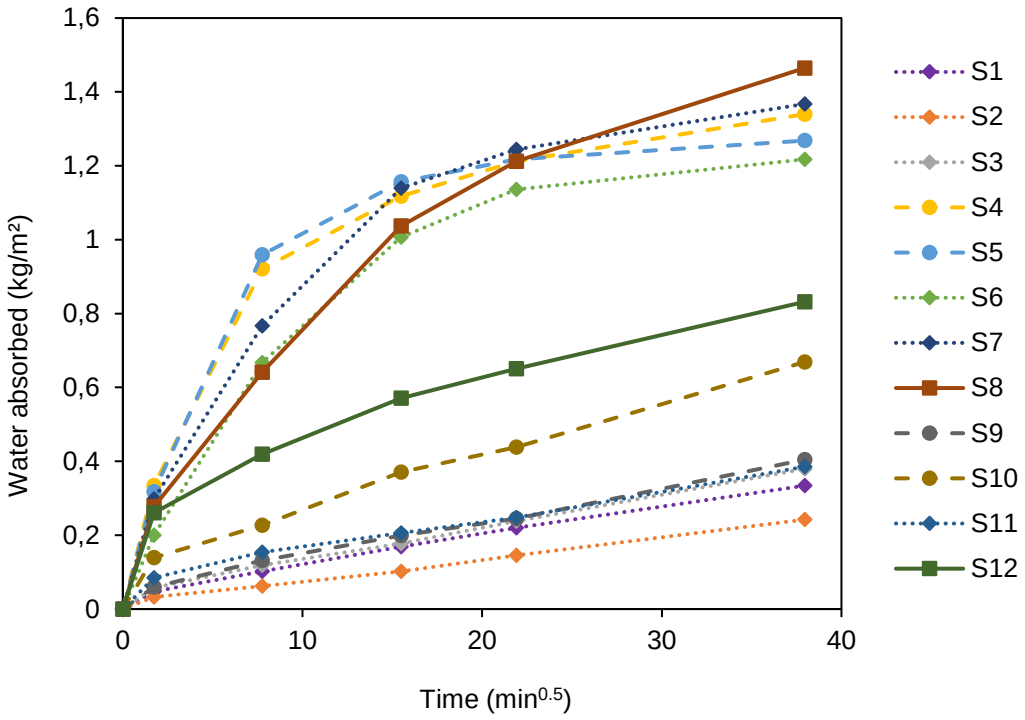

Figure 3. Capillary water absorption curves of the ETICS

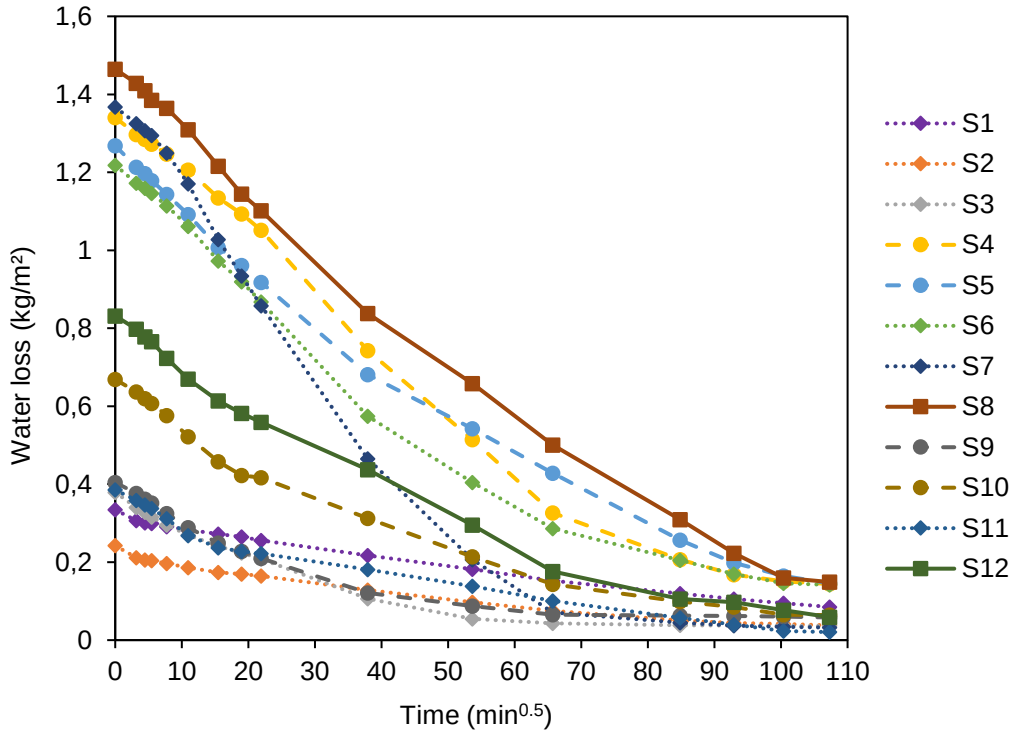

Figure 4. Drying curves of the ETICS

Table 4. Water resistance test results

System	Capillary water absorption and drying						Water vapor permeability			Karsten tubes		
	Water absorbed [kg/m^2]			C [kg/(m^2.min$^{0.5}$)]	DR1 [kg/(m^2.h)]	DR2 [kg/(m^2.h$^{0.5}$)]	ETICS (S)	Thermal Insulation (TI)	Rendering System (RS)	Water absorbed [cm^3]		C_{abs} [kg/(m^2.min$^{0.5}$)]
	3 min	1 h	24 h				μ [-]	μ [-]	Sd [m]	1 h	2 h	
S1	0.048 ± 0.005	0.102 ± 0.006	0.334 ± 0.013	0.027 ± 0.003	0.0032	0.0214	65.75	42.45	1.12	0.08 ± 0.07	0.09 ± 0.09	0.02 ± 0.01
S2	0.033 ± 0.006	0.062 ± 0.001	0.242 ± 0.006	0.019 ± 0.004	0.0030	0.0197	65.22		1.15	0.08 ± 0.09	0.10 ± 0.12	0.02 ± 0.02
S3	0.058 ± 0.002	0.118 ± 0.002	0.379 ± 0.004	0.034 ± 0.001	0.0068	0.0396	66.40		1.19	0.15 ± 0.06	0.23 ± 0.09	0.03 ± 0.01
S4	0.335 ± 0.026	0.921 ± 0.091	1.339 ± 0.032	0.193 ± 0.015	0.0172	0.1195	16.28	8.86	0.54	0.69 ± 0.16	1.14 ± 0.14	0.16 ± 0.04
S5	0.318 ± 0.014	0.959 ± 0.046	1.268 ± 0.008	0.184 ± 0.008	0.0151	0.0989	16.78		0.54	1.59 ± 0.46	2.13 ± 0.73	0.36 ± 0.10
S6	0.199 ± 0.057	0.667 ± 0.051	1.217 ± 0.156	0.115 ± 0.033	0.0169	0.1099	32.63	35.81	-	2.48 ± 0.38	3.45 ± 0.68	0.56 ± 0.09
S7	0.298 ± 0.018	0.767 ± 0.082	1.367 ± 0.009	0.172 ± 0.010	0.0242	0.1528	42.20		0.58	1.96 ± 0.11	3.35 ± 0.45	0.44 ± 0.03
S8	0.277 ± 0.001	0.641 ± 0.012	1.465 ± 0.034	0.159 ± 0.001	0.0168	0.1136	6.73	1.90	0.31	0.53 ± 0.13	0.88 ± 0.17	0.12 ± 0.03
S9	0.059 ± 0.002	0.132 ± 0.001	0.404 ± 0.011	0.034 ± 0.001	0.0066	0.0399	12.06	14.07	-	0.21 ± 0.03	0.35 ± 0.04	0.05 ± 0.01
S10	0.139 ± 0.017	0.227 ± 0.032	0.669 ± 0.058	0.081 ± 0.009	0.0095	0.0619	25.49		0.54	0.19 ± 0.05	0.29 ± 0.10	0.04 ± 0.01
S11	0.084 ± 0.002	0.154 ± 0.006	0.385 ± 0.025	0.049 ± 0.001	0.0051	0.0335	48.94	39.83	0.59	0.21 ± 0.13	0.33 ± 0.17	0.05 ± 0.03
S12	0.261 ± 0.012	0.419 ± 0.006	0.832 ± 0.044	0.151 ± 0.007	0.0111	0.0773	24.43	2.74	0.99	0.16 ± 0.09	0.21 ± 0.13	0.04 ± 0.02

C – capillary water coefficient; DR1 – drying rate 1; DR2 – drying rate 2; μ - water vapor diffusion resistance coefficient; Sd – equivalent air thickness; (-) – impossible to obtain the value due to inconsistencies in the results; C_{abs} – water absorption coefficient

Concerning capillary water absorption, all the systems present average values of absorbed water that are lower than 1 kg/m^2 at 1 h testing, thus in accordance with ETAG 004 [9] requirements and confirming their ETA. Nevertheless, for systems S4 and S5 the values of absorbed water at 1 h surpass the ETAG 004 [9] threshold if the standard deviation is considered.

The highest level of capillary absorption for all specimens is registered in the first hour of test (with a significant increase in the first 3 min), followed by a decrease in the rate of water absorption of most systems. Even though, the systems still slowly absorb water and a full saturation is not achieved after 24 h. Griciute et al. [39] obtained similar results testing four ETICS' systems, differing on the type of paint applied in the FC (acrylic, silicate, mineral, and silicone).

The highest value of water absorbed at 1 h is obtained for S5 (0.959 kg/m^2), with ICB TI, cement-resin BC and acrylic-based FC, followed by S4 (0.921 kg/m^2), with ICB TI and finished with a lime-based mortar. These systems are among those that obtained the highest values of capillary water coefficient (C), together with S7 and S8 (Table 4). Systems S7 and S8 have the same cement-based BC, similar acrylic-based FC and different TI (EPS for S7 and MW for S8). S8 is among the systems with higher values of both water absorption at 3 min testing and C. Nevertheless, it is interesting to note that S8 water absorption rate starts decreasing immediately after the initial 3 min, resulting in a lower value of water absorption during the 3 min-1 h test period when compared to S4 and S5. The water absorption rate of S8 increased again after 1 h, whereas on the other hand, S4 and S5 water absorption rate decreased after 1 h (Figure 3). At the end of the test (24 h), S8 has a higher value of absorbed water when compared to S4 or S5. These inversions of variation can be related to the different relative behaviors of the RS layers of each system. The use of an acrylic paint [4] can contribute to the lower water absorption of S5 when compared to S4, which also presents a thicker RS layer [40,41].

On the other hand, system S8, followed by S7, has the highest value of water absorption at 24 h. These systems have different TI (MW for S8 and EPS for S7), slightly differ in the composition of the FC layer and have similar RS thicknesses (Table 1). System S2 presents the lowest values of capillary water absorption, as well as the lowest C value (Table 4). When comparing the capillary water coefficients of S2 and S3, which have the same cement-resin BC and very similar FC composition, it is possible to observe a reduction of 44% in the value of C for S2, which can be attributed to the additional acrylic paint layer (Table 1). Similar results were found by Sadauskiene et al. [4], where a decrease of 59% in the value of C was observed by increasing the thickness of the applied acrylic paint from 0.08 to 0.24 mm. However, these values were obtained when testing

only the exterior RS and not the whole ETICS' systems. In fact, Griciute et al. [39] separately tested the whole ETICS' system and the RS and obtained higher results of capillary water absorption for the whole system.

When comparing systems S9 and S10, which have the same BC and TI, a considerably lower C value (around 138%) is observed for S9, which is finished with a waterborne silicate paint, when compared to S10 (acrylic-based paint in the FC). In fact, the potassium silicates of the S9 coating (both the key-coat and the paint) physic-chemically bonds (silification) to the calcium and other inorganic mineral matter of the base coat [42]. Thus, the base coat and the finishing coat end up as a single compound and/or with a strong adhesion, providing improved water repellency properties to the system S9. Polymer coating (S10), on the other hand, physically adhere to the substrate and form an interface; in fact, the formation of acrylate-siloxane copolymer (hybrid polyacrylic–polysiloxane structure) can provide water-repellency (due to the methyl groups), antimicrobial growth inhibition and enhanced adhesion properties [43-45]. Thus, the acrylic film is not chemically bonded to the base coat of S10, justifying its slightly higher water absorption, when compared to that of S9 with silicate-based paint.

System S12 presents higher values of water absorption and C, when compared to S11. As these systems present the same RS composition (cement-based BC and acrylic-based FC), this is possibly due to the influence of the TI, that differs between systems (EPS for S11 and MW for S12). In fact, MW presents hydrophilic properties that allow fast liquid water transport [6,46], whereas EPS has an internal closed pore structure, despite absorbing small amounts of water in the water permeable spaces between sintered beads [47,48]. These results can indicate that water achieved the TI layers, possibly altering their thermal resistance and compromising the systems in-service performance. Similar results were obtained for S6 and S8, with similar RS composition (cement-resin BC and acrylic-based FC) and different TI material (EPS for S6 and MW for S8), with S8 presenting an increase of 38% in the value of C when compared to S6. Even so, as mentioned before, all these systems meet ETAG 004 [9] requirement concerning capillary water absorption at 1 h.

In general, it can be stressed that some expectable trends are not verified. As an example, systems with EPS as TI, cement-based BC and acrylic FC could be expected to have the lowest water absorption rates, and this is verified for S1, S2, S3 and S11, however, not for S6 and S7. On the other hand, systems with ICB as TI, hydraulic-lime-based BC and FC would be thought to have relatively high-water absorption rates: this is verified for S4, but not in the case of S9 and S10. These findings evidence that the base materials used for each layer can be engineered in order to present enhanced water protection properties.

Regarding the drying kinetics, S7 (with EPS TI, cement-resin BC and acrylic-based FC) presents the highest values of DR1 and DR2, meaning that this system has high liquid water transport to the surface of the specimen (DR1), followed by high water vapor evaporation (DR2) [49]. Systems S4, S5, S6, and S8 present very similar DR's values, either considering DR1 or DR2. In this case, a maximum decrease of 12% and 17% was reported when comparing DR1 and DR2, respectively and for systems S4 (ICB as TI and finished with a lime-based mortar) and S5 (ICB as TI, natural hydraulic lime-based BC and acrylic-based FC). The lowest values of both DR1 and DR2 were obtained for system S2, followed by S1, S3, and S11. All these systems have EPS as TI, cement-based BC and acrylic-based FC. Interestingly, these results are in accordance with the values obtained in the capillary water absorption test. In fact, systems that absorb more water are generally those that dry faster, and a linear correlation indicating a determination coefficient (R^2) of 0.83 was obtained between DR2 and C (Figure 5).

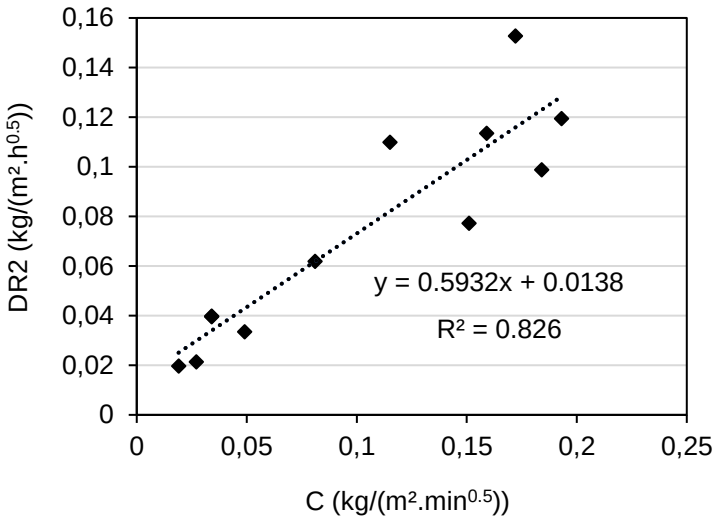

Figure 5. Correlation between ETICS drying rate 2 (DR2) and capillary water coefficient

3.2. Water vapor permeability

Table 4 presents the results of water vapor permeability (WVP) in terms of water vapor diffusion resistance coefficient (μ) for the whole ETICS´ system and for the thermal insulation, as required by ETAG 004 [9], and equivalent air thickness (Sd) for the rendering system (RS). All tested systems met ETAG 004 [9] requirements, i.e. Sd is not higher than 2 m (for systems with EPS) or 1 m (for systems with MW). The ETAG does not define an Sd threshold for ETICS using ICB, however, assuming the most severe requirement (Sd < 1 m), systems with ICB also verify this threshold value.

System S8 has the lowest μ value (6.73), followed by S4 (16.28), and S5 (16.78). However, these systems are among those presenting also the highest values of capillary water coefficient (Table 4). In fact, ETICS are constantly exposed to weathering agents and should therefore have low C values in order to regulate water intake. Simultaneously, the systems should also have high water vapor permeability (low μ) with the aim of improving moisture evaporation from the building envelope, thus decreasing possible long-term problems related to water accumulation [50]. Conversely, systems S1, S2, S3, and S11 present the highest μ values (Table 4). These systems, however, also present the lowest C and DR's values (Table 4). Similar results were reported in other studies [4,51].

Nevertheless, a different trend is observed when considering some of the systems. System S7, for example, presents higher C than S8, but also higher μ. This fact does not contribute to an adequate water vapor permeability of the system, thus increasing the risk of internal condensation [52,53]. S7 and S8 have the same cement-based BC, very similar acrylic-based FC (Table 1), and different thermal insulation material (EPS for S7; MW for S8). The higher water vapor diffusion resistance obtained for S7, when compared to S8, can be explained either by the distribution of pores in the rendering system of the ETICS, that directly affects water adsorption [54], or by the hydrophilic/hydrophobic matrix of the thermal insulation material [6,8,55], as seen in Section 3.1. In fact, the μ value of the TI of S7 (EPS, with 35.81) is significantly higher than the μ value of the TI of S8 (MW, with 1.90), which may explain the differences obtained in the μ value of the whole ETICS. When comparing silicate-based (S9) and acrylic-based (S10) coatings, the higher μ (i.e. lower water vapor diffusion) of S10 is justified by the dense polymeric structure (hybrid polyacrylic–polysiloxane structure) and high hydrophobicity of the methyl groups [43,44], whereas the more porous silicate coatings favor the dissipation of the internal moisture [42].

When comparing the μ of the TI of the different systems, the highest values are obtained for EPS (S1-S3, S6-S7, S11), followed by ICB (S4-S5, S9-S10) and then MW (S8, S12). Similar results can be found in literature [6,8,56].

The highest values of the equivalent air thickness (Sd) of the RS are obtained for S1, S2, and S3. As in the case of capillary water absorption results, the application of an additional layer of acrylic paint in S2 (marked as (b) in Table 1) promoted less water adsorption when compared to S3. The same trend was observed by Sadauskiene et al. [57] and Sadauskiene et al. [4].

3.3. Water absorption under low pressure with Karsten tubes

The Karsten tube test results are presented in Table 4 and Figure 6.

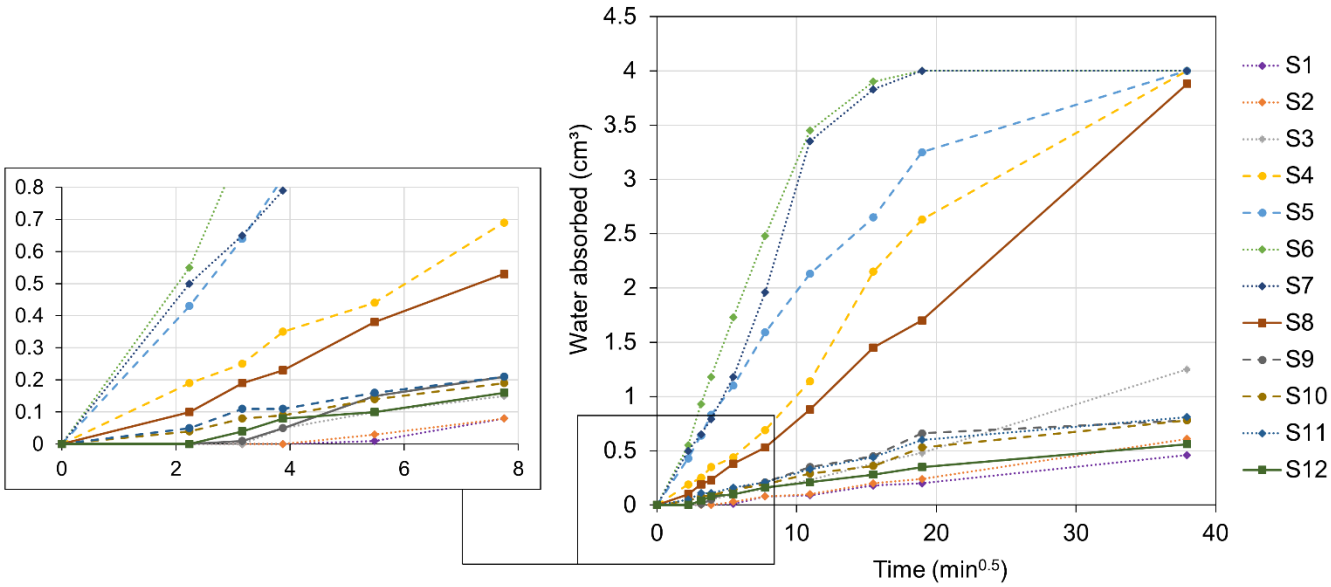

Figure 6. Water absorption curves using the Karsten tube test

Systems S1, S2, and S3, with EPS as TI, cement-resin BC and acrylic-based FC, obtained the lowest water absorption, either considering the 1- or 2-h test results. These systems also obtained the lowest values of the C_{abs} at 1 h, ranging between 0.02 kg/(m^2.min$^{0.5}$) and 0.03 kg/(m^2.min$^{0.5}$). These results are in accordance with the capillary water absorption results (Table 4), as these systems also obtained the lowest C values in the range 0.019-0.034 kg/(m^2.min$^{0.5}$).

Conversely, systems S5 (ICB as TI, natural hydraulic lime-based BC and acrylic-based FC), S6 and S7 (both with EPS TI, cement-based BC and similar acrylic-based FC) presented the highest water absorption results, both considering the 1- or 2-h test results and the C_{abs}. The results are partially in agreement with the results of the capillary water absorption test, as systems S5 and S7 are among those that obtained the highest values of both capillarity water absorption at 1 h and C (Table 4). However, the results obtained for S6 are higher than expected, if considering the ones obtained for the capillary absorption test. The differences in such results can be attributed to the adherence between the tube and the surface of the system, as well as differences in roughness along the surface [75], or even the presence of some micro-cracking [34].

3.4. Color and gloss

Figure 7 shows a comparison of the colorimetric coordinates by plotting the luminosity (L*) and chroma (C^*_{ab}) and b* and a* coordinates. All ETICS' surfaces generally present low luminosity, with system S5 presenting the lowest result (71.71) and system S9 the highest (83.13). Systems S1, S2 and S9 have the lowest chroma and thus the less saturated color.

Most of the systems present a greyish coloration, with a tendency towards yellow (+b* results), which is slightly higher in the case of S8 and S12, both having MW as TI. In any case, the a* value is close to zero for all systems, thus indicating no green or red shades in the systems.

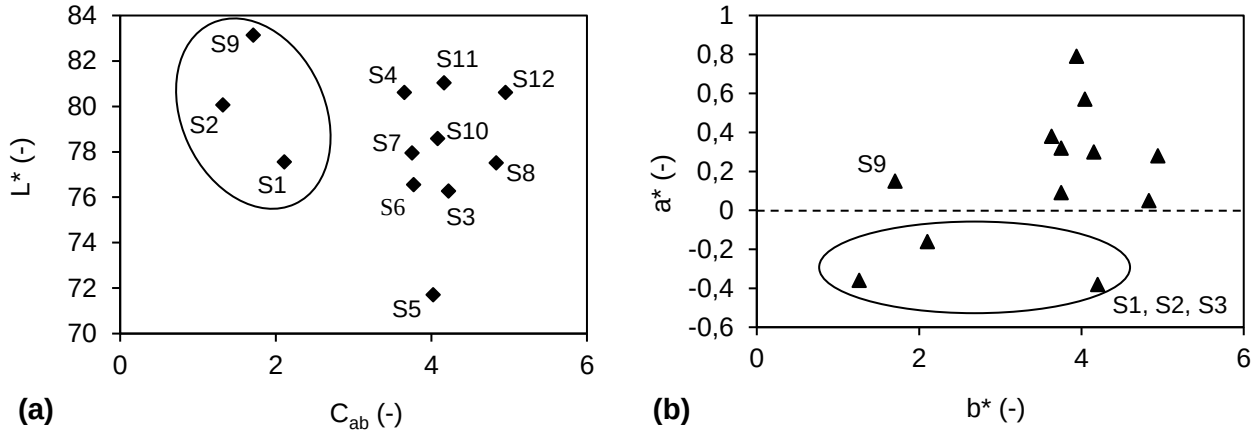

Figure 7. Comparison between L* and C^*_{ab} (a) and between b* and a*for ETICS

When comparing the different systems, it can be noticed that S1 to S3 (acrylic-based FC) are the only systems presenting negative values of a* (Figure 7b), which indicates a slight green component. For systems S4 and S5, both with ICB as thermal insulation, it can be noted a difference in L* values, attributed to the difference in their finishing coat composition (lime-based and acrylic-based, respectively). Systems S6 and S8, although with different compositions (Table 1), have similar chromatic coordinates. S10 to S12, both with the same acrylic-based finishing coat, have similar color, although system S10 has lower chroma. On the other hand, system S9, finished with a water-based silicate paint, has even higher L* and lower C^*_{ab}, if compared to S10 or S12 (both finished with an acrylic-based paint), being thus closer to an ideal white color.

When considering specular gloss, it can be noted that for all sets very low values of surface gloss (< 2.5 GU) were measured. Moreover, those values (Figure 8) are in agreement with color coordinates, meaning that luminosity (L* coordinate) and chroma (C^*_{ab}) vary with specular gloss. In fact, systems S1 and S2 have similar gloss, whereas S3 has significant lower values, when compared to S1 and S2. Interestingly, systems S6, S7,

and S8 have similar GU values, whereas S5 has both the lowest L* coordinate and gloss. Conversely, system S4, finished with a lime-based mortar, presents higher value of gloss, which doubles that obtained for system S5 (acrylic-based FC). Ultimately, systems S10 to S12 have similar gloss values; however, the values obtained for S10 slightly differ from the others.

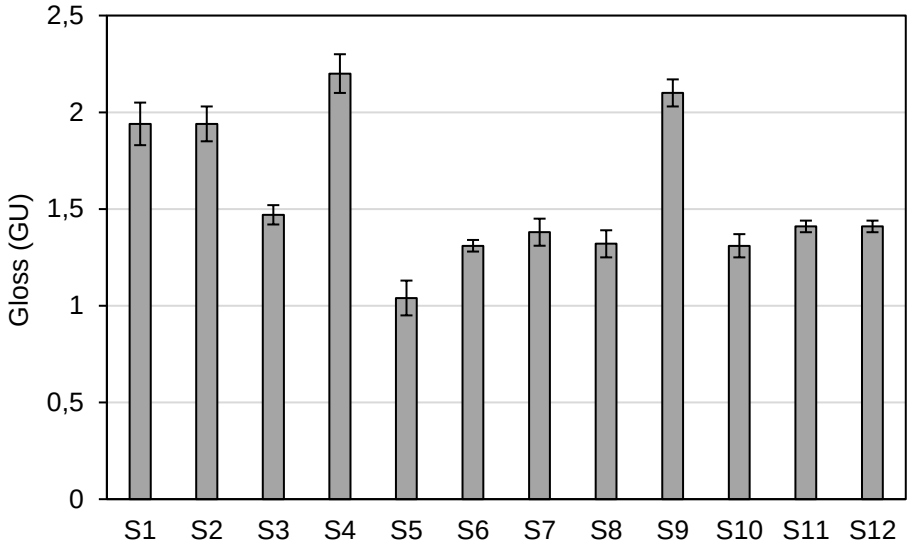

Figure 8. Average results and relative standard deviation of specular gloss for ETICS

3.5. Roughness

The results of surface roughness are presented in Figure 9.

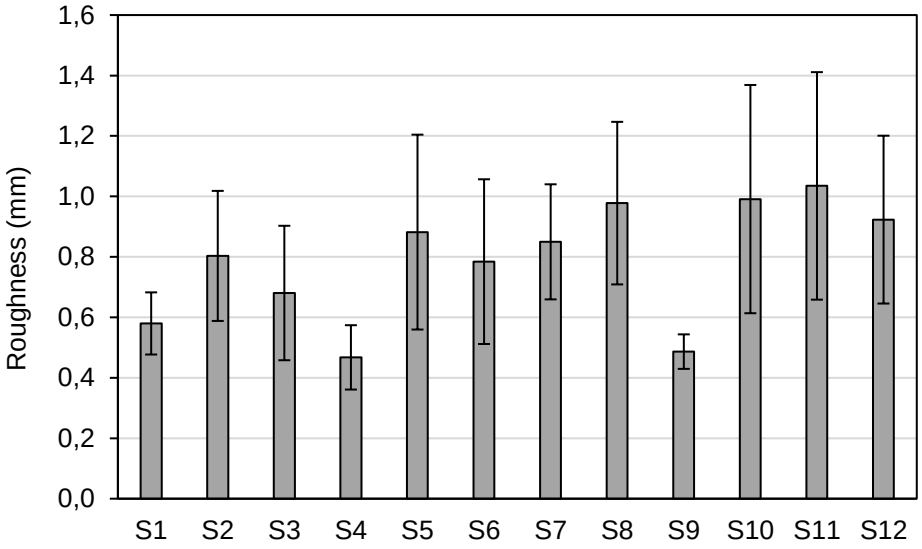

Figure 9. Average results and relative standard deviation of surface roughness for ETICS

Systems S1, S4 and S9 have the lowest roughness values of all tested systems. When comparing systems S1 to S3, which have the same thermal insulation and base coat composition and slightly differ in the finishing

coat (Table 1), it can be noted that systems S2 and S3 present higher values, due to the use of a coarser finishing coat, when compared to S1. Systems S5 to S8, although with different composition, show similar roughness values. Systems S4 and S9 are those with the lowest values of surface roughness. The values obtained for S4 can be attributed to the use of a thin lime-based layer as finishing coat, while those obtained for S9 are justified by the application of a water-based silicate paint. The remaining systems, which have an acrylic paint in the finishing coat, present higher values of surface roughness.

3.6. Thermal conductivity

Figure 10 and Table 5 show the results of thermal conductivity of the insulation material of each system for their dry state and two different moisture states, as described in Section 2.2.3. As expected, an increase of the thermal conductivity with moisture content was obtained for all the tested systems, regardless of the thermal insulation material used (EPS, ICB or MW). In fact, several authors (i.e. [7,8]) reported a linear growth correlation between thermal conductivity and moisture content for different building materials.

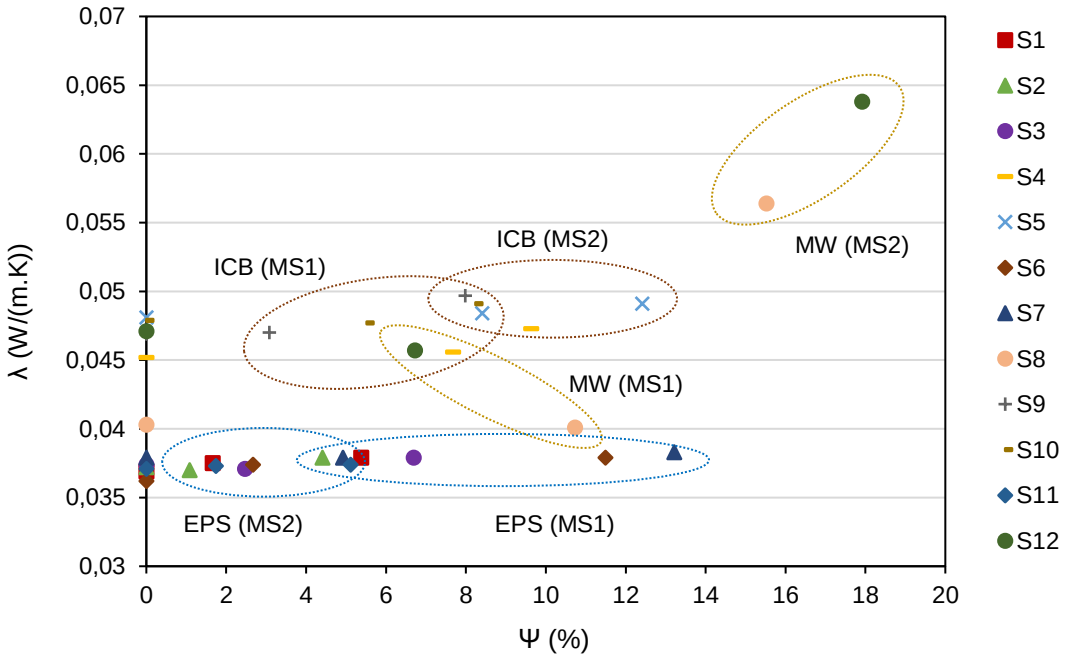

Figure 10. Thermal conductivity of the TI as a function of moisture content

Table 5. Thermal conductivity results of the insulation material

System (Type of TI)	Dry state (DS)	Moisture state 1 (MS1)			Moisture state 2 (MS2)		
	λ [W/(m.K)]	Ψ [%]	λ [W/(m.K)]	Variation [%]	Ψ [%]	λ [W/(m.K)]	Variation [%]
S1 (EPS)	0.0369	5.38	0.0379	2.71	1.66	0.0375	1.62

S2 (EPS)	0.0372	4.41	0.0379	1.88	1.08	0.0374	0.54
S3 (EPS)	0.0374	6.69	0.0379	1.34	2.47	0.0375	0.27
S4 (ICB)	0.0452	7.68	0.0456	0.88	9.63	0.0473	4.65
S5 (ICB)	0.0481	8.41	0.0484	0.62	12.41	0.0491	2.08
S6 (EPS)	0.0362	11.49	0.0379	4.69	2.67	0.0374	3.31
S7 (EPS)	0.0379	13.21	0.0383	1.06	4.92	0.0379	0
S8 (MW)	0.0403	10.73	0.0405	0.50	15.52	0.0564	39.95
S9 (ICB)	0.0469	3.08	0.0470	0.21	7.98	0.0497	5.97
S10 (ICB)	0.0479	5.51	0.0482	0.62	8.24	0.0491	2.51
S11 (EPS)	0.0371	5.11	0.0374	0.81	1.74	0.0373	0.54
S12 (MW)	0.0417	6.72	0.0457	9.59	17.92	0.0638	52.99
TI – thermal insulation; λ – thermal conductivity; Ψ – moisture content; Variation: increase in comparison to the dry state							

Regarding the systems with EPS as thermal insulation, a slight increase in thermal conductivity values between the dry state (λ_{DS}) and moisture state 1 (λ_{MS1}) was obtained. Nevertheless, the results at moisture state 2 (λ_{MS2}) are always slightly lower than those obtained at MS1. This trend can indicate that there is a certain reversibility in the insulation wetting process for systems with EPS. In other words, even if moisture achieves the insulating layer, it induces no significant variation on its thermal capacity. This can be explained by the internal closed pore structure of EPS, as stated in Sections 3.1 and 3.2, as well as by the high resistance to water penetration (both in the liquid and vapor phase) obtained for the EPS systems (Table 4). However, results confirm that the thermal conductivity is always affected by moisture content, as also confirmed by other authors (i.e. [6,58,59]). Concerning the systems with ICB as thermal insulation, an increase in the values of thermal conductivity with moisture content was obtained, both among λ_{DS} and λ_{MS1}, and λ_{MS1} and λ_{MS2}. The highest value of increase was obtained for S9 (5.74%). However, Tadeu et al. [60] concluded that for an ICB uncoated wall, moisture along the ICB is only high when the outer moisture is high and remains that way for a long period of time. This can be explained by the rather slow process of moisture diffusion within the ICB. In fact, the values of water vapor diffusion resistance coefficient (μ) obtained for ICB are considerably lower than those obtained for EPS, however, significantly higher than those obtained for MW.

For the systems with MW as thermal insulation, it was observed a noticeable increase in the values of thermal conductivity with moisture content, both between λ_{DS} and λ_{MS1}, and between λ_{MS1} and λ_{MS2}. The highest value was obtained for system S8 (40.65%). This is attributed to the hydrophilic properties of the mineral wool, presenting very high-water vapor permeability (Table 4), thus allowing thermal conductivity to increase

extremely fast with increasing moisture content [6]. Abdou and Budawi [61] also measured the thermal conductivity of several MW samples at different moisture content and concluded that thermal conductivity is affected by moisture content but also by the wetting/drying cycles over time. Furthermore, it is essential to note, however, that system S8 was the one presenting the highest capillary water absorption at 24 h (Table 4) and that a variation of 38% between the value of C obtained for S6 (EPS) and S8 (MW) was observed (Section 3.1). Thus, the values of thermal conductivity measured for S8 at MS2 confirm that water really achieved the TI layer and altered its thermal resistance.

For these reasons, it is of fundamental importance to guarantee that ETICS finishing coats present enough hydrophobicity (improved liquid water resistance and high water vapor permeability) throughout the system service life, avoiding that the moisture content at the insulation/base coat/finishing coat interfaces remain high over a long period of time. This is critical in the case of systems with MW insulation, which can absorb significantly higher water amount, when compared to EPS and ICB systems, inducing a higher increase of the thermal conductivity. Proper maintenance actions are thus necessary, applying a new finishing coat if needed. The application of water-repellent products on the ETICS' surface helps reducing water absorption [62]. Another possibility to minimize the effect of the presence of water in increasing the thermal conductivity of the MW is to provide some hydrophobic substances to the MW composition [46]. Another important aspect to be considered, and especially in the MW systems, is to avoid micro-cracking of the RS, as it would allow a quick water penetration.

3.7. Biological susceptibility to moulds

Results of the average rate of biological susceptibility of the ETICS' surface finishing layer show that no growth was detected during or at the end of the test. The validity of the test was confirmed by the results obtained for the Controls, all rated as 4 at the end of the 4-week testing (Figure 11). The fact that no growth occurred for any ETICS' surface can be explained either by the presence of biocide on the finishing coat or by the high levels of pH of some systems finishing coats. In fact, previous studies showed that pH values close or higher than 10 can inhibit mould growth [38,63]. Nevertheless, the ETICS considered in this work are newly produced, unaltered sound systems, which were not subjected to any kind of accelerated aging or weathering procedures.

When analyzing the average rate results of mould growth for the insulation materials (Figure 11), significant mould growth was obtained for the ICB samples at the end of the test (all rated as 2 or more). For EPS samples, mould growth was considerably lower, with some samples presenting only traces of growth after 4 weeks of incubation, whereas MW samples presented traces of growth since the first week of observations.

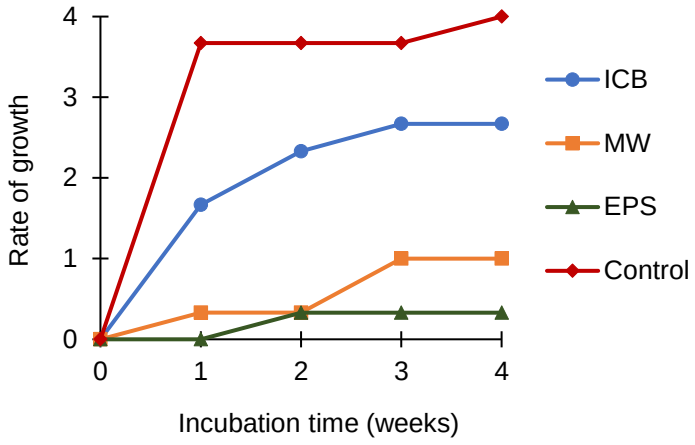

Figure 11. Average rate of mould growth for the TI materials

ICB samples presented the most intense mould growth of all TI materials as cork is a natural organic material composed of suberin, lignin and polysaccharides (cellulose and hemicellulose) [64]. Organic or organic-based materials are more vulnerable to fungal deterioration since they provide ample nutrients, through their composition, contributing to fungal growth [37,65].

On the other hand, MW and EPS samples generally presented a good resistance to mould attack, always having a rate of growth lower or equal to 1 (Figure 11). Concerning MW, a fibrous material made from inorganic materials such as molten glass, stone or slag, the susceptibility to mould growth is naturally lower than that of organic materials [37,65] though still recorded in the present study (Figure 12). Regarding EPS, composed of pre-expanded polystyrene beads, the resistance to fungal growth is noteworthy (Figure 12), which is in accordance with the results obtained by Jerábková and Tesarová [66].

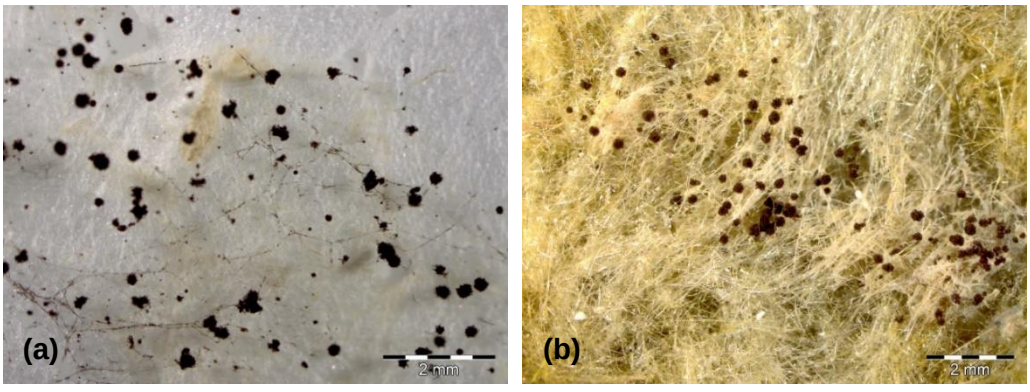

Figure 12. *A. niger* growth on (a) EPS and (b) MW samples after 4 weeks of incubation

However, as stated above, all the systems as a whole presented suitable performance concerning mould attack, showing an adequate capacity of the RS to protect the TI layer.

3.8. Performance parameters

3.8.1. Water transport properties

The results obtained in the water resistance tests allowed the definition of performance parameters for the analyzed sound ETICS. The comparison between the capillary water coefficient (C), drying rate 2 (DR2) and water vapor diffusion resistance coefficient (μ) of the systems is presented in Figure 13.

Different trends can be observed (Figure 13). A first group with similar values is defined by systems S1 to S3, from the same manufacturer and with the same BC (cement-based) and TI (EPS) compositions. For these systems, the results show that the lower the water absorption (C), the higher the water vapor resistance (μ), and the lower the drying rate in vapor form (DR2).

Systems S4 (ICB as TI and finished with a lime-based mortar) and S5 (ICB as TI, natural hydraulic lime-based BC and acrylic-based FC), produced by the same manufacturer, have a similar trend, despite having different FC composition (Table 1). In this case, again, the lower the water absorption, the greater the water vapor resistance, and the lower the drying rate in vapor form. When compared to systems S1 to S3, S4 and S5 present higher C and DR2, but significantly lower μ.

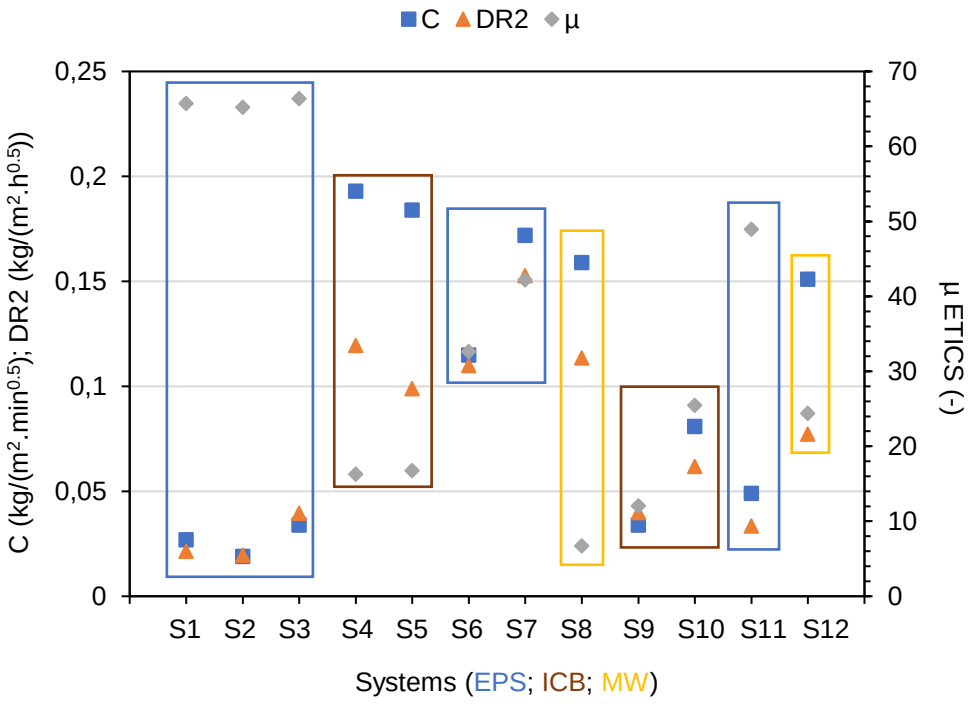

Figure 13. Comparison between C, DR2 and μ for ETICS, where the performance of the systems with different TI is framed in blue (EPS), brown (ICB) and orange (MW)

Systems S6 and S7 (both with EPS as TI, cement-based BC and acrylic-based FC), and S9 and S10, present similar trends, where the higher the C and the DR2, the greater the μ. However, S7 and S10 have higher C and μ, compared to S6 and S9, respectively. Therefore, the moisture transport properties of S7 and S10 can hinder a proper "breathability" of the system, increasing the risk of internal condensation [52,53]. It can be concluded that, at equivalent TI (ICB), a system composed of a combination of silicate-based paint and hydraulic lime-based BC (S9) has more beneficial moisture transport properties (i.e. low C and μ), if compared to a system composed of a combination of acrylic-based paint and hydraulic lime-based BC (S10). However, the same materials can probably be engineered in order to enhance their performance.

A further performance group is composed of systems S8 and S12, both with MW as thermal insulation, cement-based BC and similar acrylic-based FC. However, their DR2 and μ have opposite trends. Finally, the trend registered for system S11 (EPS as TI, cement-based BC and acrylic-based FC) is somehow comparable to that obtained for systems S1 to S3, although S11 has higher C and lower μ.

The results obtained in the water resistance tests also allowed the definition of recommendations for the evaluation of the performance of sound ETICS (Table 6). These recommendations can be used in combination with the requirements already defined in ETAG 004 [9].

Table 6. Recommendations for the performance of sound ETICS

Test	Recommendations
Water absorption by capillarity	The results of capillary absorption at 1 h and 24 h shall be presented and the water absorbed at 1 h should be < 1 kg/m^2 (in accordance with ETAG 004 recommendations). For systems with MW as thermal insulation, significant increases of thermal conductivity of the insulation in the presence of water were registered. Therefore, for these systems it is recommended the adoption of an absorbed water maximum threshold of 0.5 kg/m^2 at 24 h.
Drying capacity	A high correlation between the drying rate and the capillary water coefficient should be obtained. The correlation presented in Figure 5 between C and DR2 can be used as reference, due to its significant linear coefficient of determination (R^2=0.83).
Water vapor permeability	The value of the water vapor diffusion resistance coefficient shall be presented for both the thermal insulation, as recommended by ETAG 004, and the entire system. The latter value is relevant to compare systems with similar thermal insulation (same thickness), and different finishing.
Water absorption under low pressure (Karsten tube)	The Karsten tube test provides significant results and can be used as a complementary test for the liquid water resistance assessment, by comparing these results with those of capillary absorption test, and also for future comparison with in-situ tests. This test may also be used to detect micro-cracking and it may thus be very useful to assess systems performance after artificial or natural aging. Following European recommendations and LNEC test methods, the results of absorbed water at 1- and 2-h should be presented.

3.8.2. Surface properties

The correlation among the different surface properties is presented in Figure 14.

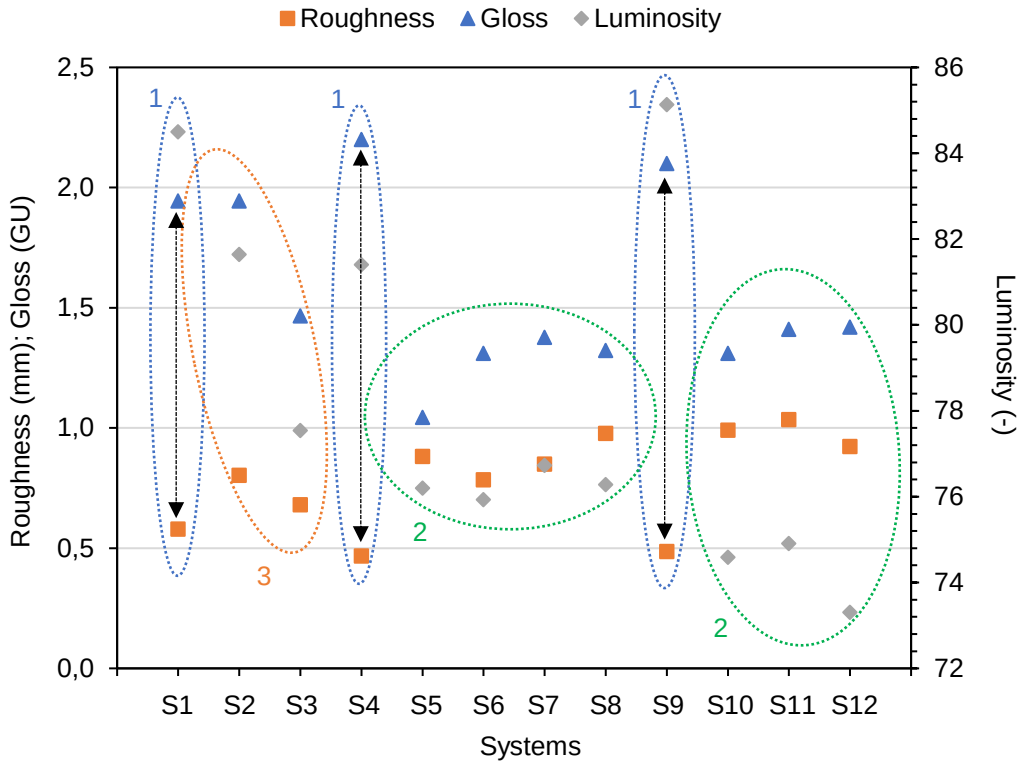

Figure 14. Comparison between roughness, gloss and luminosity for ETICS, and identification of three groups

In general, three different trends can be observed in the results. A first group consists of systems S1 (acrylic-based FC), S4 (lime-based RS) and S9 (silicate-based FC), which have low surface roughness (i.e. flat finishing coats, with inclusion of thin mineral aggregates or additives), which promotes higher gloss and luminosity. In fact, as reported in other research [67,68], low values of surface roughness confer remarkable light reflection, which leads to higher gloss. Interestingly, system S4 has the lowest surface roughness and the highest capillary water coefficient. As a matter of fact, the high surface roughness can significantly contribute to higher hydrophobicity [69].

A second group is composed of systems S5 to S8 and S10 to S12, which have similar trends. For these systems, higher roughness values (mostly due to the incorporation of coarse siliceous aggregates in the finishing coat), and lower gloss and L* color coordinate values were observed, when compared to the previous group. Ultimately, system S2 has higher roughness than S3, but also greater gloss and color.

Gloss reduction and discoloration are among the first symptoms of coating degradation [70], whereas surface roughness can significantly affect the surface hydrophobicity and biological development [17,21,71]. For these reasons, the evaluation of gloss, color and roughness should also be included in ETICS inspection protocols.

4. Conclusions

In this study, the moisture transport properties, the surface properties and the bio-susceptibility of 12 commercially available sound ETICS were assessed. The influence of the moisture content variation on the thermal conductivity of the insulation layer of ETICS was also investigated. The experimental results allowed the definition of performance parameters for sound ETICS, which can be used in combination with the requirements defined in ETAG 004.

The current work contributed to the evaluation of the efficiency and durability of ETICS considering an integrated analysis of their performance and stressing the importance of a holistic view for the correct evaluation of these systems.

Results showed that all systems have suitable moisture transport properties, accomplishing the ETAG 004 requirements. Generally, systems that absorb more water (higher C in the range 0.019-0.193 kg/(m^2.$min^{0.5}$)) are those that dry faster (higher DR2 in the range 0.0197-0.1195 kg/(m^2.$h^{0.5}$) and lower μ (between 6.73 and 66.40)). It is worth noting that, when increasing the thickness of the applied acrylic paint finishing coat (e.g. systems S2 and S3, with EPS thermal insulation and cement-resin base coat), a significant decrease (44%) of the water absorption can be obtained. Moreover, the use of silicate-based finishing coat (S9) can also control the moisture transport properties, with lower values of water absorption and water vapor diffusion resistance, when compared to acrylic-based finishing coat (S10). Additionally, high values of water absorption were obtained for systems with similar rendering system and different thermal insulation. Significant increases (up to 38%) were obtained for systems with hydrophilic mineral wool as thermal insulation. However, it was also noticed that high performance rendering systems (base coat and finishing coat) may provide good protection to the thermal insulation layers and thus confer good water performance to the systems as a whole, even in the case of hydrophilic thermal insulation materials.

It can be concluded that systems with high water absorption (e.g. with natural hydraulic lime-based base coat; with MW as thermal insulation) should have high drying and vapor permeability. Otherwise, anomalies linked to the presence of water (e.g. cracks, stains, biocolonization) might affect the long-term durability of ETICS.

Furthermore, results showed that the thermal conductivity of the thermal insulation increased with moisture content, especially for the MW. The results indicate that water achieved the thermal insulation layer, altering its thermal resistance and compromising the system in-service performance. Hence the importance of providing low wettability and thus hydrophobicity to the ETICS finishing coat throughout the system service life. The use of waterproofing treatments or additives to the ETICS can be useful strategies to control the moisture transport properties of the systems.

Additionally, although ETICS presented no growth on the finishing coat, the thermal insulation materials presented some bio-susceptibility. These results clearly highlight the need for regular maintenance actions including bio-susceptibility testing.

Finally, the monitoring of gloss, color and roughness is important to identify and understand the performance of ETICS. Results showed that low surface roughness promotes higher gloss and luminosity and lower hydrophobicity (higher C value). Technical data sheets, as well as inspection and maintenance protocols, should consider these surface properties.

Further tests are ongoing to verify the long-term durability of the systems when exposed to natural and artificial aging cycles and, ultimately, to contribute towards the development and implementation of ETICS with improved performance and durability in the urban environment.

Acknowledgments

The authors acknowledge the support given by the Portuguese Foundation for Science and Technology (FCT) within research project PTDC/ECI-EGC/30681/2017 (WGB_Shield – Shielding building' façades on cities revitalization. Triple resistance for water, graffiti and biocolonization of external thermal insulation systems). The authors also acknowledge Saint-Gobain Weber, CIN and Secil for the materials supply.

References

[1] Malanho, S., Veiga, M.R. (2020) Bond strength between layers of ETICS – Influence of the characteristics of mortars and insulation materials. *Journal of Building Engineering*, 101021. https://doi.org/10.1016/j.jobe.2019.101021

[2] Gonçalves, M., Simões, N., Serra, C., Flores-Colen, I. (2020) A review of the challenges posed by the use of vacuum panels in external insulation finishing systems. *Applied Energy*, 114028. https://doi.org/10.1016/j.apenergy.2019.114028

[3] Pasker, R. (2015) The European ETICS market – Facts & figures. In: European ETICS Forum.

[4] Sadauskiene, J., Stankevicius, V., Bliudzius, R., Gailius, A. (2009) The impact of the exterior painted thin-layer render's water vapour and liquid water permeability on the moisture state of the wall insulating system. *Construction and Building Materials*, 23, 2788-2794. https://doi.org/10.1016/j.conbuildmat.2009.03.010

[5] Clarke, J.A., Yaneske, P.P. (2009) A rational approach to the harmonization of the thermal properties of building materials. *Building and Environment*, 44, 2046-2055. https://doi.org/10.1016/j.buildenv.2009.02.008

[6] Jerman, M., Cerný, R. (2012) Effect of moisture content on heat and moisture transport and storage properties of thermal insulation materials. *Energy and Buildings*, 53, 39-46. https://doi.org/10.1016/j.enbuild.2012.07.002

[7] Gomes, M.G., Flores-Colen, I., Manga, L.M., Soares, A., de Brito, J. (2017) The influence of moisture content on the thermal conductivity of external thermal mortars. *Construction and Building Materials*, 135, 279-286. http://dx.doi.org/10.1016/j.conbuildmat.2016.12.166

[8] D'Alessandro, F., Baldinelli, G., Bianchi, F., Sambuco, S., Rufini, A. (2018) Experimental assessment of the water content influence on thermo-acoustic performance of building insulation materials. *Construction and Building Materials*, 158, 264-274. https://doi.org/10.1016/j.conbuildmat.2017.10.028

[9] EOTA (2013) Guideline for European technical approval of external thermal insulation composite systems (ETICS) with rendering. Brussels. ETAG 004.

[10] Anastaselos, D., Giama, E., Papadopoulos, A.M. (2009) An assessment tool for the energy, economic and environmental evaluation of thermal insulation solutions. *Energy and Buildings*, 41, 1165-1171. https://doi.org/10.1016/j.enbuild.2009.06.003

[11] Fernandes, C., de Brito, J., Cruz, C.O. (2016) Architectural integration of ETICS in building rehabilitation. *Journal of Building Engineering*, 5, 178-184. https://doi.org/10.1016/j.jobe.2015.12.005

[12] Barreira, E., Freitas, V.P. (2013) Experimental study of the hygrothermal behaviour of External Thermal Insulation Composite Systems (ETICS). *Building and Environment*, 63, 31-39. https://doi.org/10.1016/j.buildenv.2013.02.001

[13] Amaro, B., Saraiva, D., de Brito, J., Flores-Colen, I. (2013) Inspection and diagnosis system of ETICS on walls. *Construction and Building Materials*, 47, 1257-1267. https://dx.doi.org/10.1016/j.conbuildmat.2013.06.024

[14] Simona, P.L., Spiru, P., Ion, I.V. (2017) Increasing the energy efficiency of buildings by thermal insulation. *Energy Procedia*, 128, 393-399. https://doi.org/10.1016/j.egypro.2017.09.044

[15] Luján, S.V., Arrebola, C.V., Sánchez, A.R., Benito, P.A., Cortina, M.G. (2019) Experimental comparative study of the thermal performance of the façade of a building refurbished using ETICS, and quantification of improvements. *Sustainable Cities and Society*, 51, 101713. https://doi.org/10.1016/j.scs.2019.101713

[16] Johansson, S., Wadsö, L., Sandin, K. (2010) Estimation of mould growth levels on rendered façades based on surface relative humidity and surface temperature measurements. *Building and Environment*, 45, 1153-1160. https://doi.org/10.1016/j.buildenv.2009.10.022

[17] D'Orazio, M., Cursio, G., Graziani, L., Aquilanti, L., Osimani, A., Clementi, F., Yéprémian, C., Lariccia, V., Amoroso, S. (2014) Effects of water absorption and surface roughness on the bioreceptivity of ETICS compared to clay bricks. *Building and Environment*, 77, 20-28. http://dx.doi.org/10.1016/j.buildenv.2014.03.018

[18] Uygunoglu, T., Özgüven, S., Çalis, M. (2016) Effect of plaster thickness on performance of external thermal insulation cladding systems (ETICS) in buildings. *Construction and Building Materials*, 122, 496-504. https://doi.org/10.1016/j.conbuildmat.2016.06.128

[19] Steinbauer, V., Kaufmann, J., Zurbriggen, R., Bühler, T., Herwegh, M. (2017) Tracing hail stone impact on external thermal insulation composite systems (ETICS) – An evaluation of standard admission impact tests by means of high-speed-camera recordings. *International Journal of Impact Engineering*, 109, 354-365. https://doi.org/10.1016/j.ijimpeng.2017.07.016

[20] Sulakatko, V., Lill, I., Liisma, E. (2015) Analysis of on-site construction processes for effective external thermal insulation composite systems (ETICS) installation. *Procedia Economics and Finance*, 21, 297-305. https://doi.org/10.1016/S2212-5671(15)00180-X

[21] Barberousse, H., Ruot, B., Yéprémian, C., Boulon, G. (2007) An assessment of façade coatings against colonisation by aerial algae and cyanobacteria. *Building and Environment*, 42, 2555-2561. https://doi.org/10.1016/j.buildenv.2006.07.031

[22] Johansson, P., Ekstrand-Tobin, A., Bok, G. (2012) Laboratory study to determine the critical moisture level for mould growth on building materials. *International Biodeterioration & Biodegradation*, 73, 23-32. https://doi.org/10.1016/j.ibiod.2012.05.014

[23] CEN (2013) Conservation of Cultural Heritage – Test methods – Determination of drying properties. European Committee for Standardization. EN 16322:2013, Brussels, Belgium

[24] CEN (2004) Methods of Test for Mortar for Masonry. Part 19: Determination of Water Vapour Permeability of Hardened Rendering and Plastering Mortars. European Committee for Standardization. EN 1015-19:2004, Brussels, Belgium

[25] LNEC FE Pa 39 (2002) Wall coatings. Water absorption test under low pressure. LNEC FE PA 39.1, Lisbon, Portugal (in Portuguese)

[26] RILEM (1980) Water absorption under low pressure, Pipe method. Test Nº II.4. Recommandations provisoires. RILEM TC 25-PEM, 201-202.

[27] CEN (2013) Conservation of Cultural Heritage – Test methods – Measurement of water absorption by pipe method. European Committee for Standardization. EN 16302:2013, Brussels, Belgium

[28] ASTM (2015) Calculation of color tolerances and color differences from instrumentally measured color coordinates. ASTM International. ASTM D2244:2015, Pennsylvania, USA.

[29] ASTM (2000) Standard practice for determination of graffiti resistance. ASTM International. ASTM D6578-00, Pennsylvania, USA.

[30] ASTM (2014) Standard test method for thermal conductivity of plastic by means of transient line-source technique. ASTM International. ASTM D5930-09:2014, Pennsylvania, USA

[31] ISOMET 2114 (2011) Thermal properties analyze – User's guide version 120712. Applied Precision

[32] ASTM (2017) Determining the resistance of paint films and related coatings to fungal defacement by accelerated four-week agar plate assay. ASTM International. ASTM D5590-17:2017, Pennsylvania, USA

[33] ASTM (2019) Standard test method for determining fungi resistance of insulation materials and facings. ASTM International. ASTM C1338-19:2019, Pennsylvania, USA

[34] Hendrickx, R. (2013) Using the Karsten tube to estimate water transport parameters of porous building materials. *Materials and Structures*, 46, 1309-1320. https://doi.org/10.1617/s11527-012-9975-2

[35] Gomes, M.G., Flores-Colen, I., da Silva, F., Pedroso, M. (2018) Thermal conductivity measurement of thermal insulating mortars with EPS and silica aerogel by steady-state and transient methods. *Construction and Building Materials*, 172, 696-705. https://doi.org/10.1016/j.conbuildmat.2018.03.162

[36] Santos, T., Nunes, L., Faria, P. (2017) Production of eco-efficient earth-based plasters: Influence of composition on physical performance and bio-susceptibility. *Journal of Cleaner Production*, 167, 55-67. http://dx.doi.org/10.1016/j.clepro.2017.08.131

[37] Hoang, C.P., Kinney, K.A., Corsi, R.L., Szaniszlo, P.J. (2010) Resistance of green building materials to fungal growth. *International Biodeterioration & Biodegradation*, 64, 104-113. https://doi.org/10.1016/j.ibiod.2009.11.001

[38] Verdier, T., Coutand, M., Bertron, A., Roques, C. (2014) A review of indoor microbial growth across building materials and sampling and analysis methods. *Building and Environment*, 80, 136-149. https://doi.org/10.1016/j.buildenv.2014.05.030

[39] Griciute, G., Bliudzius, R., Norvaisiene, R. (2013) The durability test method for External Thermal Insulation Composite System (ETICS) used in cold and wet climate countries. *Journal of Sustainable Architecture and Civil Engineering*, 1:2. http://dx.doi.org/10.5755/j01.sace.1.2.2778

[40] Norvaisiene, R., Griciute, G., Bliudzius, R., Ramanauskas, J. (2013) The changes of moisture absorption properties during service life of external thermal insulation composite system. *Materials Science*, 19:1. https://dx.doi.org/10.5755/j01.ms.19.1.3834

[41] Maia, J., Ramos, N.M.M., Veiga, R. (2018) Evaluation of the hygrothermal properties of thermal rendering systems. *Building and Environment*, 144, 437-449. https://doi.org/10.1016/j.buildenv.2018.08.055

[42] Sakka, S. (2016) History of the sol-gel chemistry and technology. In: Handbook of Sol-Gel Science and Technology. Springer International Publishing, Dordrecht, Netherlands

[43] Kozakiewicz, J., Ofat, I., Trzaskowska, J. (2015) Silicone-containing aqueous polymer dispersions with hybrid particle structure. *Advances in Colloid and Interface Science*, 223, 1-39. https://doi.org/10.1016/j.cis.2015.04.002

[44] Wojciechowski, K., Kaczorowski, M., Mierzejewska, J., Parzuchowski, P. (2018) Antimicrobial dispersions and films from positively charged styrene and acrylic copolymers. *Colloids and Surfaces B: Biointerfaces*, 172, 532-540. https://doi.org/10.1016/j.colsurfb.2018.09.009

[45] Khanjani, J., Hanifpour, A., Pazokidarf, S., Zohuriaan-Mehr, M.J. (2020) Waterborne acrylic-styrene/PDMS coatings formulated by different particle sizes of PDMS emulsions for outdoor applications. *Progress in Organic Coatings*, 141, 105267. https://doi.org/10.1016/j.porgcoat.2019.105267

[46] Jiricková, M., Cerný, R. (2006) Effect of hydrophilic admixtures on moisture and heat transport and storage parameters of mineral wool. *Construction and Building Materials*, 20, 425-434. https://doi.org/10.1016/j.conbuildmat.2005.01.055

[47] Gnip, I.Y., Kersulis, V., Vejelis, S., Vaitkus, S. (2006) Water absorption of expanded polystyrene boards. *Polymer Testing*, 25, 635-641. https://doi.org/10.1016/j.polymertesting.2006.04.002

[48] Maaroufi, M., Abahri, K., Hachem, C.E., Belarbi, R. (2018) Characterization of EPS lightweight concrete microstructure by X-ray tomography with consideration of thermal variations. *Construction and Building Materials*, 178, 339-348. https://doi.org/10.1016/j.conbuildmat.2018.05.142

[49] Brito, V., Gonçalves, T.D., Faria, P. (2011) Coatings applied on damp buildings substrates: performance and influence on moisture transport. *Journal of Coatings Technology and Research*, 8, 513-525. https://doi.org/10.1007/s11998-010-9319-5

[50] Posani, M., Veiga M.R., Freitas V.P. (2019) Towards resilience and sustainability for historic buildings: a review of envelope retrofit possibilities and a discussion on hygric compatibility of thermal insulations. *International Journal of Architectural Heritage.* https://doi.org/10.1080/15583058.2019.1650133

[51] Ramanauskas, J., Stankevicius, V. (1998) Weather durability of external wall thermal insulation system with thin-layer plaster finish. *Statyba*, 4, 206-213. https://doi.org/10.1080/13921525.1998.10531406

[52] Mandilaras, I., Atsonios, I., Zannis, G., Founti, M. (2014) Thermal performance of a building envelope incorporating ETICS with vacuum insulation panels and EPS. *Energy and Buildings*, 85, 654-665. https://doi.org/10.1016/j.enbuild.2014.06.053

[53] Pereira, C., de Brito, J., Silvestre, J.D. (2018) Contribution of humidity to the degradation of façade claddings in current buildings. *Engineering Failure Analysis*, 90, 103-115. https://doi.org/10.1016/j.engfailanal.2018.03.028

[54] Xiong, H., Yuan, K., Wen, M., Yu, A., Xu, J. (2019) Influence of pore structure on the moisture transport property of external thermal insulation composite systems as studied by NMR. *Construction and Building Materials*, 228, 116815. https://doi.org/10.1016/j.conbuildmat.2019.116815

[55] Cai, S., Zhang, B., Cremaschi, L. (2017) Review of moisture behavior and thermal performance of polystyrene insulation in building applications. *Building and Environment*, 123, 50-65. https://doi.org/10.1016/j.buildenv.2017.06.034

[56] Schiavoni, S., D'Alessandro, F., Bianchi, F., Asdrubali, F. (2016) Insulation materials for the building sector: A review and comparative analysis. *Renewable and Sustainable Energy Reviews*, 62, 988-1011. http://dx.doi.org/10.1016/j.rser.2016.05.045

[57] Sadauskiene, J., Monstvilas, E., Stankevicius, V. (2007) The impact of exterior finish vapour resistance on the moisture state of building walls. *Technological and Economic Development of Economy*, 13, 73-82. https://doi.org/10.1080/13928619.2007.9637779

[58] Lakatos, Á. (2020) Investigation of the thermal insulation performance of fibrous aerogel samples under various hygrothermal environment: Laboratory tests completed with calculations and theory. *Energy & Buildings*, 214, 109902. https://doi.org/10.1016/j.enbuild.2020.109902

[59] Lakatos, Á., Deák, I., Berardi, U. (2018) Thermal characterization of different graphite polystyrene. *International Review of Applied Sciences and Engineering*, 2, 163-168. https://doi.org/10.1556/1848.2018.9.2.12

[60] Tadeu, A., Skerget, L., Simões, N., Fino, R. (2018) Simulation of heat and moisture flow through walls covered with uncoated medium density expanded cork. *Building and Environment*, 142, 195-210. https://doi.org/10.1016/j.buildenv.2018.06.009

[61] Abdou, A., Budaiwi, I. (2013) The variation of thermal conductivity of fibrous insulation materials under different levels of moisture content. *Construction and Building Materials*, 43, 533-544. https://doi.org/10.1016/j.conbuildmat.2013.02.058

[62] Hanus, M.J., Harris, A.T. (2013) Nanotechnology innovations for the construction industry. *Progress in Materials Science*, 58, 1056-1102. http://dx.doi.org/10.1016/j.pmatsci.2013.04.001

[63] Udawattha, C., Galkanda, H., Ariyarathne, I.S., Jayasinghe, G.Y., Halwatura, R. (2018) Mould growth and moss growth on tropical walls. *Building and Environment*, 137, 268-279. https://doi.org/10.1016/j.buildenv.2018.04.018

[64] Knapic, S., Oliveira, V., Machado, J.S., Pereira, H. (2016) Cork as building material: a review. *European Journal of Wood and Wood Products*, 74, 775-791. https://doi.org/10.1007/s00107-016-1076-4

[65] Klamer, M., Morsing, E., Husemoen, T. (2004) Fungal growth on different insulation materials exposed to different moisture regimes. *International Biodeterioration & Biodegradation*, 54, 277-282. https://doi.org/10.1016/j.ibiod.2004.03.016

[66] Jerábková, E., Tesarová, D. (2018) Resistance of various materials and coatings used in wood constructions to growth of microorganisms. *Wood research*, 63, 993-1002.

[67] Faucheu, J., Wood, K.A., Sung, L-P., Martin, J.W. (2006) Relating gloss loss to topographical features of a PVDF coating. *Journal of Coating Technology Research*, 3, 29-39. https://doi.org/10.1007/s11998-006-0003-8

[68] Xie, T., Kao, W., Sun, L., Wang, J., Dai, G., Li, Z. (2020) Preparation and characterization of self-matting waterborne polymer – An overview. *Progress in Organic Coatings*, 142, 105569. https://doi.org/10.1016/j.porgcoat.2020.105569

[69] Rutter, T., Hutton-Prager, B. (2018) Investigation of hydrophobic coatings on cellulose-fiber substrates with in-situ polymerization of silane/siloxane mixtures. *International Journal of Adhesion and Adhesives*, 86, 13-21. https://doi.org/10.1016/j.ijadhadh.2018.07.008

[70] Tilley, R. (2000) Colour and the optical properties of materials. Wiley, Chichester, England

[71] Prieto, B., Silva, B., Lantes, O. (2004) Biofilm quantification on stone surfaces: comparison of various methods. *Science of The Total Environment*, 333, 1-7. https://doi.org/10.1016/j.scitotenv.2004.05.003

[72] Mustapha, R., Zoughaib, A., Ghaddar, N., Ghali, K. (2020) Modified upright cup method for testing water vapor permeability in porous membranes. *Energy*, 195, 117057. https://doi.org/10.1016/j.energy.2020.117057

[73] CIE S014-4/E (2007) Colorimetry Part 4: CIE 1976 L*a*b* Colour Space. Commission Internationale de l'eclairage, CIE Central Bureau, Vienna, Austria.

[74] Krus, M., Rosler, D., Sedlbauer, K. (2006) New model for the hygrothermal calculation of condensate on the external building surface. In: Proc. Third International Building Physics Conference – Research in Building Physics and Building Engineering. Concordia University, Montreal, Canada, p. 329-333.

[75] Duarte, R., Flores-Colen, I., de Brito, J., Hawreen, A. (2020) Variability of in-situ testing in wall coating systems – Karsten tube and moisture meter techniques. *Journal of Building Engineering*, 27, 100998. https://doi.org/10.1016/j.jobe.2019.100998